Dalton Transactions

PAPER

View Article Online
View Journal

Cite this: DOI: 10.1039/c6dt02257j

Synthesis, characterization, biological activity, DNA and BSA binding study: novel copper(II) complexes with 2-hydroxy-4-aryl-4-oxo-2-butenoate†

Nenad Joksimović,[a] Dejan Baskić,[b] Suzana Popović,[b] Milan Zarić,[c] Marijana Kosanić,[d] Branislav Ranković,[d] Tatjana Stanojković,[e] Sladjana B. Novaković,[f] Goran Davidović,[g] Zorica Bugarčić[a] and Nenad Janković*[a]

Received 6th June 2016,
Accepted 13th August 2016

DOI: 10.1039/c6dt02257j

www.rsc.org/dalton

A serie of novel square pyramidal copper(II) complexes $[Cu(L)_2H_2O]$ (**3a–d**) with *O*,*O*-bidentate ligands [L = ethyl-2-hydroxy-4-aryl-4-oxo-2-butenoate; aryl = 3-methoxyphenyl-**2a**, (*E*)-2-phenylvinyl-**2b**, (*E*)-2-(4′-hydroxy-3′-methoxyphenyl)vinyl-**2c**, 3-nitrophenyl-**2d**, 2-thienyl-**2e**] were synthesized and characterized by spectral (UV-Vis, IR, ESI-MS and EPR), elemental and X-ray analysis. The antimicrobial activity was estimated by the determination of the minimal inhibitory concentration (MIC) using the broth microdilution method. The most active antibacterial compounds were **3c** and **3d**, while the best antifungal activity was showed by complexes **3b** and **3e**. The lowest MIC value (0.048 mg mL^{-1}) was measured for **3c** against *Proteus mirabilis*. The cytotoxic activity was tested using the MTT method on human epithelial carcinoma HeLa cells, human lung carcinoma A549 cells and human colon carcinoma LS174 cells. All complexes showed extremely better cytotoxic activity compared to cisplatin at all tested concentrations. Compound **3d** expressed the best activity against all tested cell lines with IC_{50} values ranging from 7.45 to 7.91 μg mL^{-1}. The type of cell death and the impact on the cell cycle for **3d** and **3e** were evaluated by flow cytometry. Both compounds induced apoptosis and S phase cell cycle arrest. The interactions between selected complexes (**3d** and **3e**) and CT-DNA or bovine serum albumin (BSA) were investigated by the fluorescence spectroscopic method. Competitive experiments with ethidium bromide (EB) indicated that **3d** and **3e** have a propensity to displace EB from the EB–DNA complex through intercalation suggesting strong competition with EB [K_{sv} = (1.4 ± 0.2) and (2.9 ± 0.1) × 10^4 M^{-1}, respectively]. K_{sv} values indicate that these complexes bind to DNA covalently and non-covalently. The achieved results in the fluorescence titration of BSA with **3d** and **3e** [K_a = (2.9 ± 0.2) × 10^6 and (2.5 ± 0.2) × 10^5 M, respectively] showed that the fluorescence quenching of BSA is a result of the formation of the **3d**– and **3e**–BSA complexes. The obtained K_a values are high enough to ensure that a significant amount of **3d** and **3e** gets transported and distributed through the cells.

Introduction

One of the fundamental goals in medicinal chemistry is the development of new anticancer and antimicrobial therapeutic agents. The use of metal containing compounds presents one of the most important strategies in the development of new anticancer and antimicrobial agents.[1–5]

One of the main health problems in our society, and one of the primary targets in medicinal chemistry is cancer. For a long time, platinum complexes have been at the centre of research studies as chemotherapy agents.[6–8] However, the treatment with platinum drugs is limited by several side effects such as nephrotoxicity and neurotoxicity.[9–13] The major interest in medicinal chemistry has been to develop and synthesize different non-platinum agents, with fewer side effects and/or lower cytotoxicity than platinum-based drugs.[14] A wide

[a]Faculty of Science, University of Kragujevac, Department of Chemistry, Radoja Domanovića 12, 34000 Kragujevac, Serbia. E-mail: nenad.jankovic@kg.ac.rs
[b]Centre for Molecular Medicine and Stem Cell Research, Faculty of Medical Sciences, University of Kragujevac, Svetozara Markovića 69, 34000 Kragujevac, Serbia
[c]Department of Biochemistry, Faculty of Medical Sciences, University of Kragujevac, Svetozara Markovića 69, 34000 Kragujevac, Serbia
[d]Faculty of Science, University of Kragujevac, Department of Biology and Ecology, Radoja Domanovića 12, 34000 Kragujevac, Serbia
[e]Institute of Oncology and Radiology of Serbia, Pasterova 14, 11000 Belgrade, Serbia
[f]Vinča Institute of Nuclear Science, University of Belgrade University of Belgrade, P.O. Box 522, 11001, Belgrade, Serbia
[g]Faculty of Medical Sciences, University of Kragujevac, Svetozara Markovića 69, 34000 Kragujevac, Serbia

†Electronic supplementary information (ESI) available: Copies of ^1H and ^{13}C NMR spectra of ligands and crystallographic data of **3a**. CCDC 1481900. For ESI and crystallographic data in CIF or other electronic format see DOI: 10.1039/c6dt02257j

variety of metal complexes based on cobalt,[15] gold,[16] palladium,[17] ruthenium,[18–21] osmium,[19,22,23] titanium,[24] molybdenum,[24] iridium,[25] rhodium,[26] tin[27] and copper,[28] were intensively studied as potential platinum replacements. One of the most investigated non-Pt compounds as potentially attractive anticancer agents were copper complexes.[29–31] For many years, a lot of research studies have actively investigated copper compounds based on the assumption that endogenous metals may be less toxic.[32,33] A different copper complex with ligands such as salicylaldehyde benzoylhydrazone,[34] 2-oxoquinoline-3-carbaldehyde Schiff-bases,[35] pyridoxal semicarbazone,[36] 1-adamantyl hydrazone bearing pyridine rings,[37] and 2-acetylpyridine benzoyl hydrazone[38] showed excellent cytotoxic activity on different tested cancer cell lines. It is also well known that copper(II) complexes have excellent antimicrobial activities.[39–41] In addition, copper complexes can be used as potential modulators of inflammatory and autoimmune responses.[42]

Keeping in mind these facts, we developed the synthesis of novel copper complexes with 2-hydroxy-4-aryl-4-oxo-2-butenoate (Scheme 1).

The newly-synthesized copper complexes were exposed to antimicrobial, cytotoxic evaluation and fluorescence measurements. In addition, we investigated the potential mechanism of cytotoxic activity. Fluorescence spectroscopy is an excellent experimental method for studies such as interactions between small molecules and biomacromolecules (DNA, carrier proteins, *etc.*). DNA molecules are major targets for various drugs and chemicals.[18,43–46] Generally, small molecules can interact with DNA *via* six modes: (a) electrostatic attractions with the anionic sugar-phosphate backbone of DNA, (b) interactions with the DNA major groove, (c) interactions with the DNA minor groove, (d) intercalation between base pairs *via* the DNA major groove, (e) intercalation between base pairs *via* the DNA minor groove, and (f) a threading intercalation mode.[47] Examination of the interaction of small molecules with DNA can be useful for creating highly efficient drugs[48] or to understand the toxic properties and mechanism of harmful chemicals (environmental pollutants, pesticides, *etc.*).[49–52] Serum albumins are the most abundant carrier proteins, which play an important role in the transportation and deposition of many biologically active compounds in the circulatory system.[53–55] Since the serum albumins contribute to osmotic blood pressure,[56] they can play a main role in drug transportation, disposition and efficiency.[57] A crucial fact is that the drugs and bioactive small molecules bind reversibly to albumin, which has a transport function.[58] Therefore, it is important to investigate the potential drug–protein interactions.

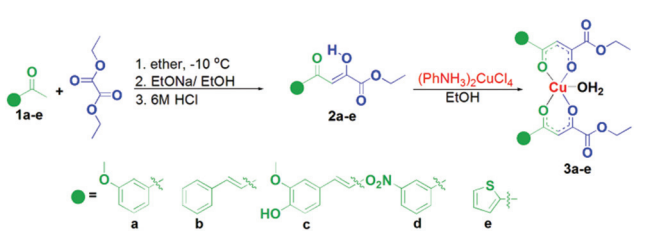

Scheme 1 Synthesis of ethyl-2-hydroxy-4-aryl-4-oxo-2-butenoate ligands **2a–e** and their copper(II) complexes **3a–e**.

Results and discussion

Synthesis and characterization

The *O*,*O*-bidentate ligands ethyl-2-hydroxy-4-aryl-4-oxo-2-butenoate **2a–e** were synthesized *via* Claisen condensation between different aromatic methyl ketones **1a–e** and diethyl oxalate under basic conditions (Scheme 1). In order to optimize reaction conditions ligand **2a** was complexed with various copper(II) salts [$CuCl_2{\cdot}2H_2O$, $Cu(CH_3COO)_2{\cdot}H_2O$ and $CuSO_4{\cdot}5H_2O$)] in boiling ethanol. However, the achieved yields were not satisfactory (29, 42 and 34% of **3a**, respectively), so we tried another synthetic strategy. Inspired by the excellent application of copper(II) salt $(PhNH_3)_2CuCl_4$ in our previous studies,[59–61] we decided to apply it in the synthesis of complexes **3a–e**. This salt yields complexes **3a–e** with ligands **2a–e** in a short reaction time (~10 min) at room temperature and the obtained yields, up to 88%, were much better than with previous copper(II) salts. One of the explanations for the improved procedure (higher yields, lower temperature and faster reaction time) with $(PhNH_3)_2CuCl_4$ is probably connected with the geometry of the $CuCl_4$ species.[62,63] All complexes are soluble in polar organic solvents [CH_3OH, 1,4-dioxane, dimethyl sulfoxide (DMSO) and dimethylformamide (DMF)] and air-stable compounds.

The IR spectra of complexes **3a–e** showed bands approximately at 1570 and 1510 cm^{-1} assigned to ν(C=C) coupled with ν(C=O) and ν(C=O) coupled with ν(C=C) respectively. The IR spectra of complexes compared to the appropriate ligand spectra showed that ν(γ-C=O) is negatively shifted by approximately 15 cm^{-1}. The presence of intense bands near 1270 cm^{-1} in the spectrum of ligands **2a–e** is the consequence of bending O–H vibrations in the plane,[64,65] while their absence in the spectra of complexes **3a–e** is caused by the coordination of the ligand to copper(II) which is followed by the deprotonation of the O–H group.

Crystal structure of 3a. The crystal structure of the Cu(II) complex determined by the X-ray diffraction analysis is presented in Fig. 1. The Cu(II) ion is placed in a nearly ideal square pyramidal environment formed by the oxygen donors from the bidentate [ethyl-2-hydroxy-4-(3-methoxyphenyl)-4-oxo-2-butenoate] ligands in the corners of the base plane and a water oxygen donor in the apex of the pyramid. By coordination to Cu(II), the organic ligands form six-membered chelate rings and display a *cis* mutual arrangement. The ligands, which coordinate as keto–enol anions, show slight variations in the lengths of four Cu–O bonds [1.914(2) to 1.927(2) Å]. As expected, the apical oxygen is placed at a longer distance from the metal center [2.371(2) Å]. The greatest deviation of angles from an idealized square pyramidal geometry is 7.2° and concerns the *trans* O4a–Cu–O3b angle of the base plane.

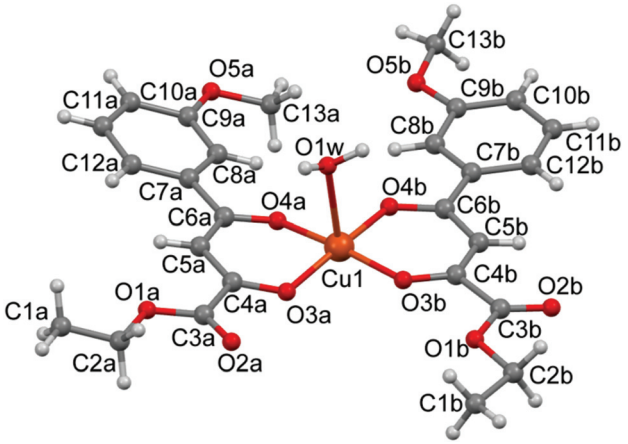

Fig. 1 X-ray molecular structure of the Cu(II) complex (**3a**).

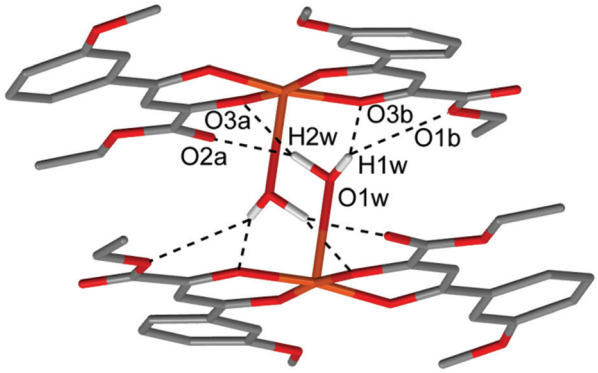

Fig. 2 Complex molecules arrange into distinct H-bonded dimers. Geometrical parameters of H-bonds are listed in Table S3 (see the ESI†). H atoms not involved in H-bonding are excluded for the sake of clarity.

Although displaying the same coordination mode the two organic ligands have a partly dissimilar molecular conformation. This is mainly expressed in the orientation of the ethyl ester functionality where the corresponding carboxyl O2 takes the *cis* or *trans* position with respect to the coordinated O3 atom in a and b ligands [torsion angles O2–C3–C4–O3 equal to 5.1(4) and −179.1(3)° in a and b, respectively]. An additional difference appears in the orientation of the methoxy moiety attached to the phenyl ring [torsion angles C8–C9–O5–C13 equal to −0.5(4) and 179.9(3)° in ligands a and b, respectively]. Despite these conformational differences, the two ligands have similar bond lengths and angles (Table S2, see the ESI†). The lengths of C–O [C4–O3 = 1.272 and C6–O4 = 1.271 Å in average] and C–C bonds [C4–C5 = 1.384 and C5–C6 = 1.405 Å in average] suggest electron delocalization within the diketone moiety. As a result, the six-membered chelate rings formed upon coordination are approximately planar. The displacement of the Cu(II) ion from the mean plane of the chelate ring somewhat differs and equals −0.158 (1) and 0.033(1) Å for ligands a and b, respectively.

In the crystal packing, the centrosymmetrically related complex molecules interconnect by O–H···O hydrogen bonds forming the distinct dimers (Fig. 2).

Within the dimer, each axial water ligand incorporates between the four O acceptors from the neighboring molecule and simultaneously forms four O–H···O hydrogen bonds. Interestingly, the above-mentioned dissimilar orientation of the ester moiety seems to allow the closer approaching of the water H-donors toward the oxygen acceptors. The bifurcated hydrogen bonds are moderately strong, with the four O···O distances in the range of 2.945(3) to 3.212(3) Å.

EPR study. The continuous-wave EPR spectrum of polycrystalline complexes of **3a–3e** at the X-band frequency (≈ 9.5 GHz) at 77 K, using Mn–ZnS as a field marker, is shown in Fig. 3.

The values of parallel ($g_{\|}$) and perpendicular ($g_{\perp}$) of the anisotropic tensor (g) from Table 1 followed the order $g_{\|} > g_{\perp} > g_e$ (g_e = 2.0023) and suggested that the $d_{x^2-y^2}$ orbital of the Cu(II) ion is the ground state for the paramagnetic electron being located in distorted sites elongated along the z-axis.[66,67] In the presented axial spectra (Fig. 3), g-values are related by the expression $G = (g_{\|} - g_e)/(g_{\perp} - g_e)$.[66] The G values ($G < 4.0$, Table 1) show that a spin–exchange interaction is present.

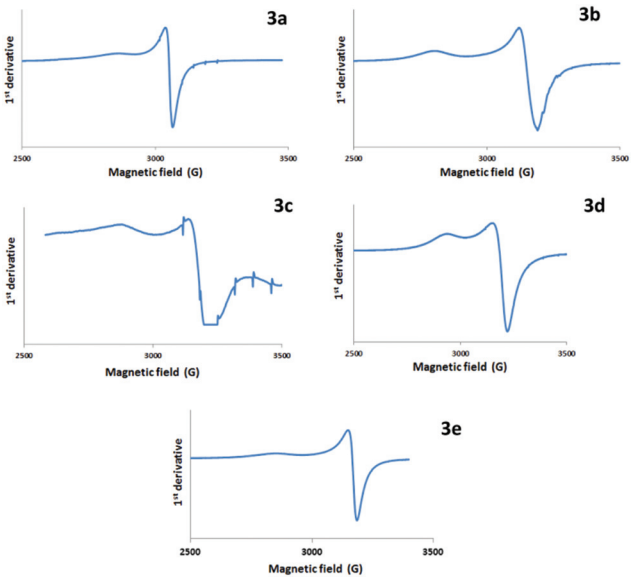

Fig. 3 EPR spectra of **3a–3e** at 77 K.

Table 1 EPR data for copper(II) complexes **3a–d**. In all cases, the standard deviation is ±0.0001

Complex	$g_{\|}$	$g_{\perp}$	G
3a	2.3389	2.1127	3.0489
3b	2.3867	2.1267	3.0900
3c	2.3343	2.1158	2.9251
3d	2.2787	2.1024	2.7612
3e	2.3537	2.1129	3.1772

Table 2 Antimicrobial activities of tested compounds **3a–e** (MIC/ mg mL^{-1}). Antibiotics: ketoconazole for fungi; streptomycin for bacteria. The values are means of three replicates. In all cases, the standard deviation is ±0.002

Compounds	**3a**	**3b**	**3c**	**3d**	**3e**	Antibiotics
Microorganism	MIC (mg mL^{-1})					
Staphylococcus aureus	0.781	0.390	0.097	0.195	1.562	0.031
Bacillus subtilis	0.781	0.781	0.097	0.390	0.781	0.016
Bacillus cereus	1.562	0.390	0.390	0.195	0.390	0.016
Escherichia coli	1.562	0.781	0.781	0.195	0.390	0.062
Proteus mirabilis	0.097	0.195	0.048	0.097	0.195	0.016
Aspergillus niger	0.390	0.390	1.562	1.562	0.781	0.156
Candida albicans	0.195	0.390	0.195	0.781	0.781	0.039
Penicillium italicum	0.781	0.390	3.125	3.125	0.390	0.156
Fusarium solani	1.562	0.390	3.125	3.125	0.195	0.156
Mucor mucedo	3.125	1.562	3.125	3.125	1.562	0.625
Trichoderma viride	1.562	0.781	1.562	3.125	0.781	0.156

Biological evaluation

Antimicrobial activities. The antimicrobial activities of the tested compounds against the test microorganisms are shown in Table 2. The tested compounds demonstrated relatively strong antimicrobial activity. The MIC for different compounds relative to the tested microorganisms ranged from 0.048 to 3.125 mg mL^{-1}. The strongest antibacterial activity was found in **3c** and **3d** components, which in very low amounts (Table 2) inhibited all the species of bacteria. The lowest measured MIC value was 0.048 mg mL^{-1} for **3c** against *Proteus mirabilis* species. These compounds also inhibited the growth of all the tested fungi but in slightly higher concentrations. **3a**, **3b** and **3d** compounds showed a similar antifungal activity with MIC values ranging from 0.195 to 3.125 mg mL^{-1}. The weaker antifungal activity was found in the **3c** and **3d** compounds.

The most sensitive, among the bacteria, was *Proteus mirabilis* while among the fungi, the most sensitive appeared to be *Candida albicans*.

The antimicrobial activity was compared with the standard antibiotics, streptomycin (for bacteria) and ketoconazole (for fungi). The results showed that the standard antibiotics had similar or stronger activity than tested samples as shown in Table 2. In a negative control, DMSO had no inhibitory effects on the tested organisms.

In these experiments, the compounds examined at the same concentrations showed a slightly stronger antibacterial than antifungal activity. These results could be expected due to the fact that numerous tests proved that bacteria are more sensitive to the antibiotic compared to fungi. The reason for different sensitivities between fungi and bacteria can be found in the different permeabilities of the cell wall. The cell wall of Gram-positive bacteria consists of peptidoglycans (murein) and teichoic acids, while the cell wall of Gram-negative bacteria consists of lipopolysaccharides and lipopolyproteins,[68] whereas the cell wall of fungi consists of polysaccharides such as chitin and glucan.[69]

Cytotoxic activity. The cytotoxicity of complexes **3a–e** against the human epithelial carcinoma (HeLa), human lung carcinoma (A549) and human colon carcinoma (LS174) cell lines was tested by the MTT [3-(4,5-dimethylthiazol-2-yl)-2,5-diphenyltetrazolium bromide] test, using cisplatin (*cis*-DDP) as the control. The results of cytotoxic activity of **3a–e** related to the tested cell lines, expressed as the IC_{50} values (μg mL^{-1}), are presented in Table 3. In addition, IC_{50} values expressed in μM are presented graphically in Fig. 4.

Table 3 Cytotoxic activity (IC_{50} values) of compounds **2a–e** and **3a–e** against human cancer cell lines and human fetal lung fibroblast cell line (MRC-5). IC_{50} values (μg mL^{-1}) were expressed as the mean ± SD determined from the results of MTT assay in three independent experiments. *cis*-DDP used as a positive control

	HeLa	LS174	A549	MRC-5
Compounds	IC_{50} (μg mL^{-1})			
2a	78.22 ± 1.55	110.57 ± 2.34	143.39 ± 3.71	—
2b	45.41 ± 0.74	55.49 ± 1.08	72.22 ± 1.43	—
2c	88.52 ± 2.31	101.87 ± 2.42	122.65 ± 3.58	—
2d	78.73 ± 1.52	156.76 ± 4.55	72.77 ± 2.06	—
2e	93.53 ± 1.78	136.14 ± 4.72	143.17 ± 2.56	—
3a	10.12 ± 1.69	8.22 ± 0.62	9.67 ± 0.59	21.22 ± 1.53
3b	9.98 ± 1.23	10.09 ± 1.02	10.15 ± 1.16	15.64 ± 1.17
3c	10.01 ± 1.15	8.65 ± 0.72	8.83 ± 0.67	11.69 ± 0.72
3d	7.91 ± 0.37	7.45 ± 0.91	7.78 ± 1.02	19.13 ± 0.44
3e	8.26 ± 0.21	7.82 ± 0.55	9.17 ± 0.13	22.55 ± 1.26
***cis*-DDP**	2.36 ± 0.28	20.38 ± 0.44	17.93 ± 0.88	4.26 ± 0.46

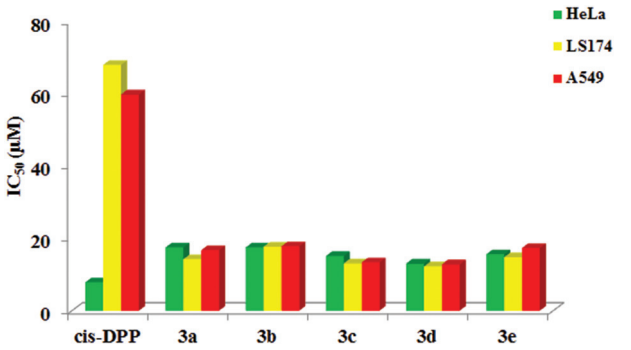

Fig. 4 Graphical representation of cytotoxic activity (IC_{50} in μM) of compounds **3a–e** against HeLa, LS174 and A549 cell lines.

As shown in the table, all complexes showed extremely high cytotoxic activity. Complex **3d** showed the best effect against HeLa, LS174 and A549 cell lines (IC_{50} = 7.91, 7.45 and 7.78 μg mL^{-1}, respectively). Furthermore, all complexes showed higher cytotoxic activity against LS174 and A549 cells compared to ***cis*-DDP** as a positive control. Comparing the results, shown in Table 3, between ligands **2a–2e** and complexes **3a–3e**, it is shown that copper plays an important role in cytotoxic activity.

In addition, the selectivity index of **3a–e** (Table 4) indicates that all compounds have better selectivity than cisplatin (up to 13 times).

Based on the achieved results of high cytotoxicity and the best selectivity (Tables 3 and 4) of compounds **3d** and **3e** we examined their effects on the cell cycle progression of A549 cells.

Effect of newly-synthesized copper complexes on apoptosis in the A549 cell line. In order to investigate the modality of **3d**- and **3e**-induced decrease in A549 cells viability, the type of cell death was evaluated by flow cytometry using Annexin V/7-AAD staining. A549 cells were treated with 10 μg mL^{-1} of **3d**, 10 μg ml^{-1} of **3e** or media alone (control) for 24 hours. Both **3d** and **3e** significantly increased the percentage of apoptotic A549 cells (52.4% and 57.32% early apoptotic; 1.32% and 0.48% late apoptotic, respectively) compared to untreated (control) cells (4.41% and 0.02%) (Fig. 5, $p < 0.001$). There were no significant differences between the percentages of necrotic cells in **3d** (0.17%) and **3e** treated A549 cells (0.21%) compared to control (0.87%). These results showed that both **3d** and **3e** in a concentration near IC_{50} induce apoptosis in over 50% of A549 cells (Fig. 5) indicating that the type of cell death induced by the tested substances is apoptosis.

Table 4 Selectivity index

	HeLa	LS174	A549
Compounds	IC_{50}(MRC-5)/IC_{50}(cell line)		
3a	2.10	2.58	2.19
3b	1.57	1.55	1.54
3c	1.17	1.35	1.32
3d	2.42	2.57	2.46
3e	2.73	2.88	2.46
***cis*-DDP**	1.81	0.21	0.24

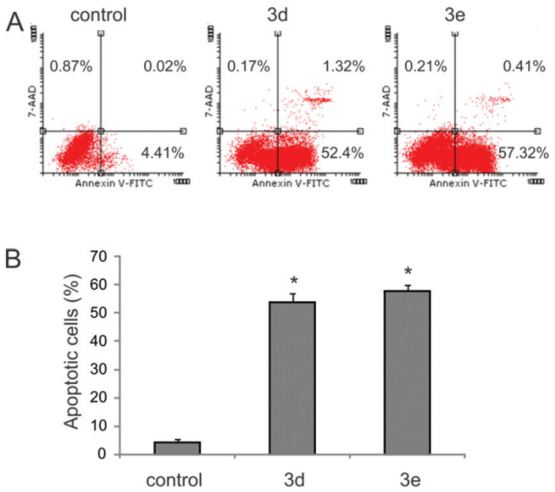

Fig. 5 Flow cytometric analysis of Annexin V-FITC/7-AAD staining. (A) Dot plots present the percentage of viable (lower left quadrant), early apoptotic (lower right quadrant), late apoptotic (upper right quadrant) and necrotic cells (upper left quadrant). (B) Percentage of apoptotic cells in control and cells treated with 10 μg mL^{-1} **3d** and **3e**.

Effect of newly-synthesized copper complexes on the cell cycle in the A549 cell line. To reveal the mechanisms underlying the decrease of viability induced by **3d** and **3e**, the effect of the tested substances on the cell cycle distribution in A549 cells was determined using flow cytometry (Fig. 6).

A 24 hour treatment of A549 cells with 10 μg mL^{-1} of **3d** resulted in a statistically significant increase in the percentage of cells accumulated in the S phase coupled with a decrease in the percentage of cells in the G0/G1 phase ($p < 0.05$). Similar results were obtained after the 24 hour treatment of A549 cells with 10 μg mL^{-1} of **3e** ($p < 0.05$) (Fig. 6). These results demonstrated that both **3d** and **3e** arrest mitosis and make the cell cycle stop at the S phase resulting in cellular apoptosis. Apoptosis and the cell cycle are directly connected.[70] The cell

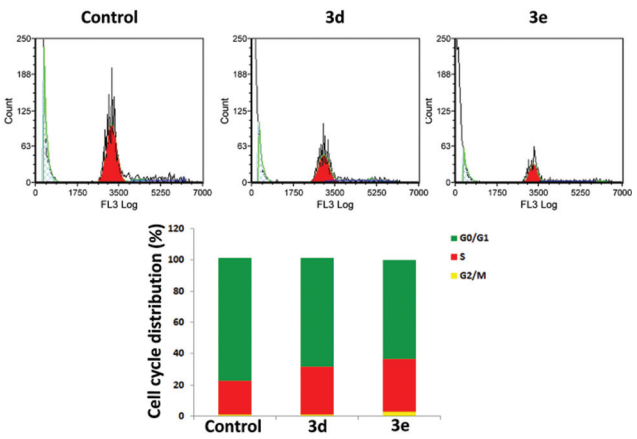

Fig. 6 Flow cytometric analysis of the cell cycle. Top: Histograms present the cell cycle distribution in untreated cells (control) and cells treated with 10 μg mL^{-1} **3d** and **3e**. Bottom: Both compounds induced similar increase in the percentage of cells in the S phase.

cycle machinery has a set of regulatory molecules that, in the case of damage, prop cell cycle arrest, affording the cell time to fix the damage. If the defect cannot be fixed, the apoptotic program gets started. Thus, the G2/M phase arrest induced by **3d** and **3e** can be a possible mechanism that triggers apoptosis. Thus, the S phase arrest induced by **3d** and **3e** points to the blockade of DNA replication as a possible mechanism that triggers apoptosis. It should be noted that apoptosis selective to the S phase cells indicates a possible inhibition of topoisomerase I.[71]

Fluorescence measurements

Fluorescence quenching on EB–DNA. Fluorescence intensity measurements of the intermolecular deactivation process of *in situ* formed complex species, between ethidium bromide (EB) and DNA (EB–DNA), were performed in the presence of **3d** and **3e** in phosphate buffer saline (PBS). The molecular fluorophore EB was particularly used since, when bound to DNA, it shows intense emission because of its strong intercalation between the neighboring DNA base pairs.[72]

The fluorescence quenching spectra of titration EB–DNA with **3d** and **3e** solutions were recorded in the range of 565–740 nm (Fig. 7). The fluorescence emission intensity at 613 and 615 nm of the EB–DNA solution showed a significant decrease (hypochromism) upon increasing the concentrations of **3d** and **3e**, respectively. In addition, the maximum wavelength of the EB–DNA was red-shifted (by about 12 nm). The observed quenching of EB–DNA species indicates competition for binding to DNA between the added complexes and EB.

The fluorescence quenching of **3d** and **3e** was described by means of the Stern–Volmer equation (1),[73] implying that the dependence of I_0/I on [Q] was examined (Fig. 7).

$$I_0/I = 1 + k_q\tau_0[Q] = 1 + K_{SV}[Q] \quad (1)$$

In eqn (1), I_0 and I are the emission intensities in the absence and presence of the quenchers, [Q] is the total concentration of the quenchers, k_q is the bimolecular quenching rate constant, and τ_0 is the average lifetime of DNA in the absence of a quencher (10^{-8} s). K_{sv} is the Stern–Volmer quenching constant whose values were obtained from the slopes of the plots of I_0/I *versus* [Q].

Table 5 The bimolecular quenching rate constant (k_q), Stern–Volmer constant (K_{sv}), and correlation coefficient (R) for the quenchers **3d** and **3e**

Compound	k_q [M^{-1} s^{-1}]	K_{sv} [M^{-1}]	R
3d	$(1.4 \pm 0.2) \times 10^{12}$	$(1.4 \pm 0.2) \times 10^{4}$	0.997
3e	$(2.9 \pm 0.1) \times 10^{12}$	$(2.9 \pm 0.1) \times 10^{4}$	0.991

Quenching parameters presented in Table 5 for **3d** and **3e** [$(1.4 \pm 0.2) \times 10^4$ and $(2.9 \pm 0.1) \times 10^4$ M^{-1}, respectively] indicate that the observed complexes have a large affinity and efficiency to substitute EB from the EB–DNA complex, and then bind strongly with DNA through intercalation.

Protein binding experiments. Investigation of the affinity of compounds **3d** and **3e** to bind to bovine serum albumin (BSA) is based on the fact that the efficiency of drugs depends on their ability to bind to carrier protein. Binding properties were investigated by using the fluorescence emission titration of BSA with **3d** and **3e** in the wavelength range of 315–465 and 300–465 nm, respectively. As can be seen in Fig. 8, the continuous decrease of the fluorescence intensity of BSA is followed by the increasing concentrations of **3d** and **3e**.

The fluorescence quenching data were examined by using eqn (2):[74]

$$\log(I_0 - I/I) = \log K_a + n \log[Q] \quad (2)$$

where I_0 and I are the emission intensities in the absence and presence of the quencher, K_a is the binding constant for **3d** or **3e**–BSA interaction, n is the number of binding sites per BSA molecule, and [Q] is the concentration of the quencher. The plots of $\log[(I_0 - I)/I]$ *versus* log[Q] are depicted in Fig. 8. The values of K_a and n were obtained from the intercept and slope

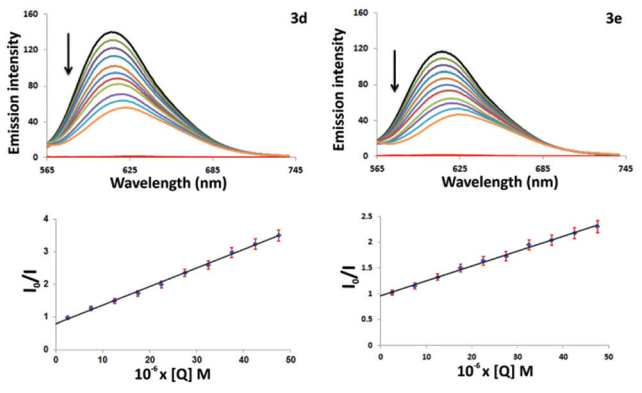

Fig. 7 Top: Emission spectra of EB bound to DNA in the absence (black lines) and presence of compounds **3d** and **3e**. The red lines denote solutions: buffer + quencher. [EB] = 47.5 μM, [DNA] = 47.5 μM; [**3c**] and [**3d**] = 0–47.5 μM; pH = 7.4; λ_{ex} = 500 nm. Bottom: Plots of I_0/I *versus* [Q].

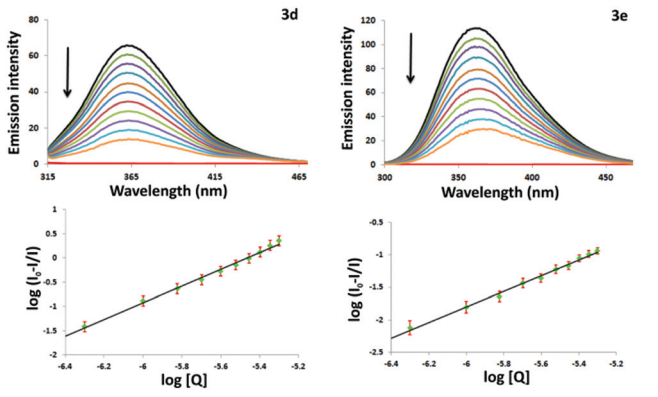

Fig. 8 Top: Emission spectra of BSA in the absence (black lines) and presence of compounds **3d** and **3e**. The red lines denote solutions: buffer + quencher. [BSA] = 2.0 μM; [**3d**] and [**3e**] = 0.0, 0.5, 1.0, 1.5, 2.0, 2.5, 3.0, 3.5, 4.0, 4.5 and 5.0; pH = 7.4; λ_{ex} = 280 nm. Bottom: Plots of $\log(I_0 - I/I)$ *versus* log[Q].

Table 6 Binding parameters (K_a and n) and the correlation coefficient (R) for the interaction of **3d** and **3e** with BSA

Compound	K_a (M^{-1})	n	R
3d	$(2.9 \pm 0.2) \times 10^6$	1.71	0.991
3e	$(2.5 \pm 0.2) \times 10^5$	1.21	0.996

of the obtained straight lines. The values of the binding parameters for **3d**- and **3e**-BSA complexes are given in Table 6.

The obtained values of K_a (Table 6) that are in the optimum range, which is considered to be 10^4–10^6 M^{-1},[75] indicate that both complexes have a great ability to bind to BSA. In addition, K_a values for **3d**–BSA and **3e**–BSA complexes show that both complexes are suitable for drug–cell interactions. In order to confirm the strong binding of **3d** or **3e** to BSA, UV/Vis spectroscopy was used. From the UV/Vis spectra (Fig. S1†), it can been seen that for a drug : BSA molar ratio of 2.5 almost all amounts of drugs bind to BSA. Thus this confirms the strong drug-to-BSA binding achieved in fluorescence measurements.

The number of binding sites of **3e** ($n \approx 1$, Table 6) points to the fact that it binds to BSA in the molar ratio of 1 : 1, while the number of binding sites ($n \approx 2$) of **3d** indicates that it binds to BSA at a molar ratio of 2 : 1. Additionally, stoichiometry in the reaction of **3d** and BSA was further tested by using the Job method of continuous variation. The obtained results showed that the maximum of the Job plot corresponds the molar ratio of **3d** : BSA approximately 2 : 1 ($X_{3d} : X_{BSA}$ = 0.65 ± 0.02 : 0.35 ± 0.02, Fig. S2†). These results confirmed that the stoichiometry of **3d** : BSA is 2 : 1.

Investigation of the formation of the copper(II)–2a complex by the Job method

A set of samples was prepared and analyzed by UV-Vis spectrophotometry after 5 h of incubation time. First, ligand **2a** and copper(II) spectra were recorded in order to evaluate the best wavelength to perform the complex absorbance measurements. The selected wavelength was 354 nm. Ligands and copper(II) do not absorb in this region, so the correction of the complex absorbance was not needed. Molar ratios of the ligands and copper(II) were: 1 : 19, 1 : 9, 1 : 5.7, 1 : 4, 1 : 3, 1 : 2.34, 1 : 1.85, 1 : 1.5, 1 : 1.2, 1 : 1, 1.2 : 1, 1.5 : 1, 1.85 : 1, 2.34 : 1, 3 : 1, 4 : 1, 5.7 : 1, 9 : 1, 19 : 1. Dependence of the measured absorbance at 354 nm and the mol fraction of **2a** is depicted in Fig. S3.† The Job plot presented in Fig. S3† showed that the complex stoichiometry is Cu^{2+} : **2a** = 1 : 2 once the plotic inflection point was observed in X_{2a} = 0.68. The stability constant K_{st} = 1.55 × 10^7 ($\log K_{st}$ = 7.19) was calculated by using eqn (3):[76]

$$\log K_{st} = 0.3522 - 2\log k + \log y_{max} - 3\log(1 - y_{max}) \quad (3)$$

Experimental

All solvents [absolute EtOH (99.8%), anhydrous diethyl ether (99.7%) and acetone (99.5%)], substrates [$CuCl_2 \cdot 2H_2O$, $Cu(CH_3COO)_2 \cdot H_2O$, $CuSO_4 \cdot 5H_2O$, aniline, vanillin, diethyl oxalate, 3-methoxyacetophenone (**1a**), 4-phenyl-3-buten-2-one (**1b**), 3-nitroacetophenone (**1d**) and 2-acetylthiophene (**1e**)], calf-thymus DNA (CT-DNA), BSA (bovine serum albumin) and reagents [sodium ethoxide, ethidium bromide (EB) and [3-(4,5-dimethylthiazol-2-yl)-2,5-diphenyltetrazolium bromide (MTT)] were purchased from Sigma. 4-(4′-Hydroxy-3′-methoxyphenyl)-3-buten-2-one (**1c**) was synthesized by the procedure described earlier.[77] Phosphate buffered saline (PBS) tablets were purchased from Fisher BioReagents. The complex salt, $(PhNH_3)_2CuCl_4$, was synthesized by the procedure described earlier.[63] A fresh solution of CT-DNA and EB in doubly distilled water was prepared in 10 mM PBS buffer at pH = 7.4. The DNA solution gave a ratio of UV absorbance at 260 nm and 280 nm (A_{260}/A_{280}) of *ca.* 1.8–1.9, indicating that the DNA was sufficiently free of proteins. CT-DNA concentration was measured by the UV absorbance at 260 nm (ε = 6600 M^{-1} cm^{-1}).[78]

Fluorescence experiments for a protein binding study

BSA solution (20 μM) was prepared in 10 mM PBS buffer at pH = 7.4 and stored in the dark at 4 °C, no longer than 3 days. The **3d**– and **3e**–BSA complexes were prepared by independently incubating a constant amount of BSA with increasing amounts of the complexes **3d** and **3e**. The molar ratios of BSA : **3d** or **3e** followed the order: 1 : 0 (control), 1 : 0.25, 1 : 0.5, 1 : 0.75, 1 : 1, 1 : 1.25, 1 : 1.5, 1 : 1.75, 1 : 2.0, 1 : 2.25, 1 : 2.5, in a total volume of 5.0 mL, pH 7.4, at 25 °C with an incubation time of 5 h. The concentration of BSA was 2.0 μM. The emission spectra were recorded between 300 and 465 nm upon excitation at 280 nm immediately after the incubation. The emission spectra of the solutions that contained only complexes (at the highest concentration) were also recorded. Appropriate blanks were used to correct the fluorescence background. All the values of absorbance measured at 250 to 500 nm for solutions that contained only complexes are sufficiently low enough (<0.05 [79]) to avoid the inner filter effect and corrections were not necessary.

Melting points (Mp) were determined on a Mel-Temp apparatus and they are uncorrected. An UV-Vis spectrum was recorded using a Perkin Elmer 35. The IR spectra were recorded using a Perkin–Elmer Spectrum One FT-IR spectrometer on a KBr pellet. Electron paramagnetic resonance measurements of solid complexes at room temperature were performed on a Bruker ESP300 spectrometer operated at the X-band frequency, using Mn–ZnS as a field marker. EPR spectra were recorded by using the following parameters: microwave frequency 9.76 GHz, microwave power 2.27 mW, attenuator 20 dB, modulation amplitude 6 Gauss and modulation frequency 100 kHz. The NMR spectra of ligands **2a–e** were recorded in $CDCl_3$ with TMS as the internal standard on a Varian Gemini 200 MHz NMR spectrometer. Mass spectrometry was performed by using a Waters Micromass Quattro II triple quadrupole mass spectrometer and MassLynx software for control and data processing. Electrospray ionization was used in the positive mode. The electrospray capillary was set at

2.5 kV and the cone at 30 V. The ion source temperature was set at 120 °C and the flow rates for nitrogen bath and spray were 500 L h^{-1} and 50 L h^{-1}, respectively. The collision energy was 15 eV. Microanalyses of C, H and N were performed on a CarloErba EA1108. The RF-1501 PC spectrofluorometer (Shimadzu, Japan) was used for fluorescence measurements.

Synthesis of ligands 2a–e

Diethyl oxalate (1.75 g, 12 mmol) and the appropriate ketones (**1a–e**, 10 mmol) were dissolved in 50 ml of anhydrous diethyl ether and cooled to −10 °C in a salt-ice bath. After reaching the temperature of −10 °C, sodium ethoxide (1.02 g, 15 mmol), which had been previously dissolved in 5 mL absolute ethanol, was added dropwise. Very quickly, during the instilment of the sodium ethoxide solution, precipitation of the sodium salt of the corresponding ligand occurred. After instilment, the reaction mixture was stirred for an additional 30 minutes at room temperature. The obtained salt was filtered, washed with anhydrous ether and dried at room temperature. Then the salt was dissolved in water (200 ml) and acidified with 6 M HCl solution to pH = 2. After acidification, voluminous precipitation of the resulting ligand occurred. The ligands were filtered, washed with water and left at room temperature to dry to yield (up to 93%). The synthesized ligands were characterized by NMR spectroscopy (^{1}H and ^{13}C spectra of ligands **2a–2e** are presented in the ESI, Fig. S4–S13†).

Synthesis of Cu(II) complexes 3a–e

The appropriate ligands **2a–e** (1 mmol) were dissolved in absolute ethanol (3 mL), then the complexing salt $(PhNH_3)_2CuCl_4$ (0.19 g, 0.5 mmol) was added. After 5–10 minutes the precipitation of the resulting complex occurred. The reaction is followed by thin-layer chromatography with chloroform as the eluent. The resulting complexes were filtered and washed with anhydrous diethyl ether. Recrystallization of complexes was done from boiling ethanol. After cooling, the complexes were precipitated, filtered, washed with diethyl ether and dried at room temperature.

3a [Cu(2a)$_2$H$_2$O]. Green crystals; yield: 81% (0.469 g); mp = 128 °C; ESI-MS: [M^+] = 580 (11%); Anal. Calcd for $C_{26}H_{28}O_{11}Cu$ (%): C 53.84 H 4.87; Found (%): C 53.96 H 4.91; IR (KBr, cm^{-1}): ν 3502, 3457, 1730, 1601, 1583, 1569, 1510, 1486, 1442, 1368, 1297, 1260, 1245, 1181, 1164, 1084, 1022, 756; UV-Vis (CH_3OH, λ_{max}/nm, (log(ε/M^{-1} cm^{-1})): 350(4.46), 289(4.25).

3b [Cu(2b)$_2$H$_2$O]. Yellow powder; yield: 65% (0.372 g); mp = 210 °C; ESI-MS: [M^+] = 572 (31%); Anal. Calcd for $C_{28}H_{28}O_9Cu$ (%): C 58.79 H 4.93; Found (%): C 58.60 H 5.01; IR (KBr, cm^{-1}): ν 3500, 3457, 1726, 1637, 1578, 1571, 1511, 1445, 1333, 1285, 1258, 1179, 1160, 1018, 863, 779; UV-Vis (CH_3OH, λ_{max}/nm, (log(ε/M^{-1} cm^{-1})): 587(2.91), 371(4.64), 328(4.50).

3c [Cu(2c)$_2$H$_2$O]. Brown crystals; yield: 78% (0.518 g); mp = 146 °C; ESI-MS: [M^+] = 664 (21%); Anal. Calcd for $C_{30}H_{32}O_{13}Cu$ (%): C 54.26 H 4.86; Found (%): C 54.36 H 4.75; IR (KBr, cm^{-1}): ν 3456, 3047, 2977, 2937, 2637, 1728, 1629, 1566, 1513, 1428, 1266, 1177, 1158, 1125, 1026, 947, 842; UV-Vis (CH_3OH, λ_{max}/nm, (log(ε/M^{-1} cm^{-1})): 404(4.71), 283(4.37).

3d [Cu(2d)$_2$H$_2$O]. Light green crystals; yield: 69% (0.420 g); mp = 236 °C; ESI-MS: [M^+] = 609 (10%); Anal. Calcd for $C_{24}H_{22}N_2O_{13}Cu$ (%): C 47.26 H 3.64 N 4.59; Found (%): C 47.39 H 3.68 N 4.63; IR (KBr, cm^{-1}): ν 3456, 3091, 2986, 1722, 1593, 1565, 1523, 1426, 1349, 1301, 1243, 1077, 1020, 716; UV-Vis (CH_3OH, λ_{max}/nm, (log(ε/M^{-1} cm^{-1})): 353(4.06).

3e [Cu(2e)$_2$H$_2$O]. Green powder; yield: 88% (0.468 g); mp = 111 °C; ESI-MS: [M^+ + Na] = 555 (14%); Anal. Calcd for $C_{20}H_{20}S_2O_9Cu$ (%): C 45.15 H 3.79; Found (%): C 45.26 H 3.85; IR (KBr, cm^{-1}): ν 3535, 3490, 3094, 2978, 1729, 1573, 1530, 1507, 1446, 1411, 1355, 1291, 1245, 1229, 1144, 1034, 1012, 775; UV-Vis (CH_3OH, λ_{max}/nm, (log(ε/M^{-1} cm^{-1})): 362(4.60), 282(4.29).

Single crystal X-ray crystallography

Single-crystal diffraction data for the Cu(II) complex (**3a**) were collected at room temperature on an Agilent Gemini S diffractometer equipped with Mo Kα radiation (λ = 0.71073 Å). Data reduction and empirical absorption corrections were performed with CrysAlisPro.[80] The crystal structure was solved by using SHELXS and refined by using SHELXL programs.[81] The hydrogen atoms attached to the C atoms were placed at the geometrically idealized positions with C–H distances fixed to 0.93, 0.97 and 0.96 Å from phenyl, methylene and methyl C atoms, respectively. The isotropic displacement parameters were set equal to $1.2U_{eq}$ and $1.5U_{eq}$ of the parent C atoms. The hydrogen atoms of the apical water ligands were located in the difference Fourier map and refined with a restrained O–H distance. The crystallographic data are listed in Table S1.† The PARST[82] and PLATON[83] programs were used to perform the geometrical calculation and the program Mercury[84] was employed for molecular graphics.

Antimicrobial activity

Microorganisms and media. The following bacteria were used as test organisms in this study: *Staphilococcus aureus* (ATCC 25923), *Bacillus subtilis* (ATCC 6633), *Bacillus cereus* (ATCC 10987), *Escherichia coli* (ATCC 25922) and *Proteus mirabilis* (ATCC 29906). All of the bacteria used were obtained from the American Type Culture Collection (ATCC). The bacterial cultures were maintained on Müller–Hinton agar substrates (Torlak, Belgrade). The fungi used as test organisms were: *Aspergillus niger* (ATCC 16888), *Candida albicans* (ATCC 10259), *Penicillium italicum* (ATCC 10454), *Mucor mucedo* (ATCC 20094), *Trichoderma viride* (ATCC 13233), and *Fusarium solani* (ATCC 36031). All of the fungi were from the American Type Culture Collection (ATCC). The fungal cultures were maintained on potato dextrose (PD) agar, except for *Candida albicans* that was maintained on Sabouraud dextrose (SD) agar (Torlak, Belgrade). All of the cultures were stored at 4 °C and subcultured every 15 days.

Bacterial inoculi were obtained from bacterial cultures incubated for 24 h at 37 °C on Müller–Hinton agar substrates and

brought up by dilution according to the 0.5 McFarland standard to approximately 10^8 CFU mL^{-1}. Suspensions of fungal spores were prepared from freshly mature (3- to 7-day-old) cultures that grew at 30 °C on a PD agar substrate. The spores were rinsed with sterile distilled water, used to determine turbidity spectrophotometrically at 530 nm, and were then further diluted to approximately 10^6 CFU mL^{-1} according to the procedure recommended by NCCLS.[85]

Minimal inhibitory concentration (MIC)

The minimal inhibitory concentration (MIC) was determined by the broth microdilution method using 96-well microtiter plates.[86] A series of dilutions with concentrations ranging from 25 to 0.012 mg mL^{-1} of the tested compounds was used in the experiment against every microorganism tested. The starting solutions of tested compounds were obtained by measuring off a certain quantity of the compounds and dissolving it in 5% DMSO. Two-fold dilutions of the compounds were prepared in a Müller–Hinton broth for bacterial cultures and a SD broth for fungal cultures. The MIC was determined with resazurin. Resazurin is an oxidation–reduction indicator used for the evaluation of microbial growth. It is a blue non-fluorescent dye that becomes pink and fluorescent when reduced to resorufin by oxidoreductases within viable cells. The boundary dilution without any changing color of resazurin was defined as the MIC for the tested microorganism at a given concentration. As a positive control of growth inhibition, streptomycin was used in the case of bacteria and ketoconazole in the case of fungi. A 5% DMSO solution was used as a negative control for the influence of the solvents.

Cytotoxic activity

Cell lines. Human epithelial carcinoma HeLa cells, human lung carcinoma A549 cells, human colon carcinoma LS174 and a non-cancerous cell line MRC-5 (human embryonic lung fibroblast) cells were obtained from the American Type Culture Collection (Manassas, VA, USA). All cancer cell lines were cultured as a monolayer in the RPMI 1640 nutrient medium, with 10% heat-inactivated (56 °C) fetal bovine serum (Sigma Chemical Co., St Louis, MO, USA) supplemented with 3 mmol L^{-1} L-glutamine, 100 mg mL^{-1} streptomycin, and 100 IU mL^{-1} penicillin. Cells were grown in a humidified atmosphere of 95% air and 5% CO_2 at 37 °C.

Treatment of cell lines. *In vitro* assay for cytotoxic activity of investigated samples was performed when the cells reached 70–80% confluence. A stock solution of samples was dissolved in the corresponding medium to the required working concentration. Neoplastic HeLa cells (5000 cells per well), A549 cells (5000 cells per well), LS174 cells (5000 cells per well) and non-cancerous MRC-5 (5000 cells per well) were seeded into 96-well microtiter plates, and 24 h later, after cell adherence, 5 different, double diluted concentrations of investigated extracts were added to the wells. Final concentrations of the samples were 200, 100, 50, 25, and 12.5 μg mL^{-1} except for the control wells, where only a nutrient medium was added. The cultures were incubated for the next 72 h.

Determination of cell survival (MTT test)

The effect on cancer cell survival was determined 72 h after the addition of extract, by the MTT test.[87] Briefly, 20 μL of MTT solution (5 mg mL^{-1} PBS) was added to each well and incubated for a further 4 h at 37 °C in 5% CO_2 and humidified air. Subsequently, 100 μL of 10% SDS was added to solubilize the formazan crystals formed from MTT after the conversion by mitochondrial dehydrogenases of viable cells. Absorbencies proportional to the number of viable cells were measured using a microplate reader (Multiskan EX, Thermo Scientific, Finland) at 570 nm. Each experiment was performed in triplicate and independently repeated at least four times.

Cell cycle analysis

A549 cells were incubated with the tested substances (10 μg mL^{-1}) or with media alone (control) for 24 h at 37 °C in an atmosphere of 5% CO_2 and absolute humidity. Cells were harvested, washed in PBS and fixed with 70% ethanol at +4 °C. Fixed cells were pelleted and finally resuspended in 1 mL PBS with RNAse A (500 μg mL^{-1}). Cells were incubated 30 minutes at 37 °C and then stained with 5 μL PI (10 mg mL^{-1} PBS). After 15 minutes incubation in the dark, samples were analysed by a flow cytometer Cytomics FC500 (Beckman Coulter). The cell cycle distribution was determined using FCS Express 5 Plus Software and the results are presented using histograms.

Determination of apoptosis/necrosis by flow cytometry

For apoptosis detection, an Annexin V-FITC/7-AAD Kit (Beckman Coulter, USA) was used. A549 cells were incubated with the tested substances (10 μg mL^{-1}) or with media alone (control) for 24 h at 37 °C in an atmosphere of 5% CO_2 and absolute humidity. Cells (attached and detached) were harvested, washed in PBS and resuspended in 500 μL of ice cold binding buffer. Cells were stained with 10 μL of Annexin V-FITC and 20 μL of 7-AAD, incubated for 15 minutes in the dark, and then 400 μL of binding buffer was added to each tube. Samples were analysed by a flow cytometer Cytomics FC500 (Beckman Coulter). Data were analyzed using Flowing Software (http://www.flowingsoftware.com/). The percentage of viable, apoptotic and necrotic cells was presented by dot plots.

Conclusions

We have developed a facile and efficient synthetic route to novel copper(II) complexes (**3a–e**) with ethyl-2-hydroxy-4-aryl-4-oxo-2-butenoate at ambient temperature. The complex salt $(PhNH_3)_2CuCl_4$ was for the first time used as a complexing reagent. Single-crystal X-ray analyses of compound **3a** showed that the ligand **2a** forms a mononuclear complex of nearly ideal square pyramidal geometry with 1 : 2 stoichiometry between copper(II) and **2a**. Antimicrobial evaluations of the novel complexes **3a–e** were investigated *via* treatment of a series of bacteria and fungi strains. The strongest antibacterial activity was found in **3c** and **3d** compounds, while the best antifungal activity was showed by **3b** and **3e**. The lowest

measured MIC value was 0.048 mg mL^{-1} found for **3c** related to the *Proteus mirabilis* species. Based on the MIC values, the most sensitive among the fungi were *Candida albicans*. The obtained results of *in vitro* cytotoxic activities indicate that compounds **3a–e** possess significant anticancer potential on various cell lines (HeLa, LS174 and A549). All complexes showed lower IC_{50} values on LS174 and A549 cell lines than the chemotherapy drug cisplatin. In addition, we found that the most active compounds **3d** and **3e** induced apoptosis in over 50% of tested cells, as verified by FITC-Annexin V and propidium iodide double staining. The cell cycle progression of A549 cells treated with both complexes showed an increase of cell population at the S phase which points to the blockade of DNA replication as a possible mechanism that triggers apoptosis. Fluorescence measurements of CT-DNA interaction with **3d** and **3e** showed that both quenchers partially replace EB from the EB–DNA complex species, and quench fluorescence intensity. The obtained quenching constants indicated that both complexes bind to CT-DNA *via* an intercalative mode. The measured values of binding constants for interaction between **3d** or **3e** and carrier protein (BSA) are in the optimum range (10^4–10^6 M^{-1}) suggesting that the formed complex species (**3d**-BSA and **3e**-BSA) are suitable for drug–cell interactions. Therefore, our results indicate that the five novel copper(II) complexes have the ability to become possible candidates for anticancer therapy.

Acknowledgements

The authors are grateful to the Ministry of Education, Science and Technological Development of the Republic of Serbia for financial support (Grant 172011). We also wish to thank Professor Dušan Milivojević for his help and support during the work on the EPR.

Notes and references

1 P. J. Sadler, *Adv. Inorg. Chem.*, 1991, **36**, 1.
2 L. Ronconi and P. J. Sadler, *Coord. Chem. Rev.*, 2007, **251**, 1633.
3 R. W.-Y. Sun, D.-L. Ma, E. L.-M. Wong and C.-M. Che, *Dalton Trans.*, 2007, **43**, 4884.
4 S. P. Fricker, *Dalton Trans.*, 2007, **43**, 4903.
5 T. W. Hambley, *Dalton Trans.*, 2007, **43**, 4929.
6 B. Lippert, *Cisplatin: Chemistry and Biochemistry of a Leading Anticancer Drug*, Wiley Interscience, 1999.
7 A. S. Abu-Surrah and M. Kettunen, *Curr. Med. Chem.*, 2006, **13**, 1337.
8 M. Arsenijevic, M. Milovanovic, V. Volarevic, D. Canovic, N. Arsenijevic, T. Soldatovic, S. Jovanovic and Z. D. Bugarcic, *Transition Met. Chem.*, 2012, **37**, 481.
9 J. T. Hartmann, L. M. Fels, S. Knop, H. Stolt, L. Kanz and C. Bokemeyer, *Invest. New Drugs*, 2000, **18**, 281.
10 J. T. Hartmann and H.-P. Lipp, *Expert Opin. Pharmacother.*, 2003, **4**, 889.
11 J. Sastry and S. J. Kellie, *Pediatr. Hematol. Oncol.*, 2005, **22**, 441.
12 R. P. Miller, R. K. Tadagavadi, G. Ramesh and W. B. Reeves, *Toxins*, 2010, **2**, 2490.
13 S. R. McWhinney, R. M. Goldberg and H. L. McLeod, *Mol. Cancer Ther.*, 2009, **8**, 10.
14 I. Ott and R. Gust, *Arch. Pharm.*, 2007, **340**, 117.
15 R. Gust, D. Posselt and K. Sommer, *J. Med. Chem.*, 2004, **47**, 5837.
16 M. Arsenijevic, M. Milovanovic, V. Volarevic, A. Djekovic, T. Kanjevac, N. Arsenijevic, S. Dukic and Z. D. Bugarcic, *Med. Chem.*, 2012, **8**, 2.
17 A. R. Kapdi and I. J. S. Fairlamb, *Chem. Soc. Rev.*, 2014, **43**, 4751.
18 D. Lazic, A. N. Arsenijevic, R. Puchta, Z. D. Bugarcic and A. Rilak, *Dalton Trans.*, 2016, **45**, 4633.
19 S. M. Meier, M. Hanif, Z. Adhireksan, V. Pichler, M. Novak, E. Jikovsky, M. A. Jakupec, V. B. Arion, C. A. Davey, B. K. Keppler and C. G. Hartinger, *Chem. Sci.*, 2013, **4**, 1837.
20 R. Trondl, P. Heffeter, C. R. Kowol, M. A. Jakupec, W. Berger and B. K. Keppler, *Chem. Sci.*, 2014, **5**, 2925.
21 B. S. Murray, L. Menin, R. Scopelliti and P. J. Dyson, *Chem. Sci.*, 2014, **5**, 2536.
22 W.-X. Ni, W.-L. Man, S.-M. Yiu, M. Ho, M. T.-W. Cheung, C.-C. Ko, C.-M. Che, Y.-W. Lam and T.-C. Lau, *Chem. Sci.*, 2012, **3**, 1582.
23 Y. Fu, M. J. Romero, A. Habtemariam, M. S. Snowden, L. Song, G. J. Clarkson, B. Qamar, A. M. Pizarro, P. R. Unwin and P. J. Sadler, *Chem. Sci.*, 2012, **3**, 2485.
24 P. M. Abeysinghe and M. M. Harding, *Dalton Trans.*, 2007, **32**, 3474.
25 L. He, Y. Li, C.-P. Tan, R.-R. Ye, M.-H. Chen, J.-J. Cao, L.-N. Ji and Z.-W. Mao, *Chem. Sci.*, 2015, **6**, 5409.
26 F.-M. Siu, I. W.-S. Lin, K. Yan, C.-N. Lok, K.-H. Low, T. Y.-C. Leung, T.-L. Lam and C.-M. Che, *Chem. Sci.*, 2012, **3**, 1785.
27 S. K. Hadjikakou and N. Hadjiliadis, *Coord. Chem. Rev.*, 2009, **253**, 235.
28 W. Zhou, X. Wang, M. Hu, C. Zhu and Z. Guo, *Chem. Sci.*, 2014, **5**, 2761.
29 F. Tisato, C. Marzano, M. Porchia, M. Pellei and C. Santini, *Med. Res. Rev.*, 2010, **30**, 708.
30 C. Marzano, M. Pellei, F. Tisato and C. Santini, *Anti-Cancer Agents Med. Chem.*, 2009, **9**, 185.
31 C. Santini, M. Pellei, V. Gandin, M. Porchia, F. Tisato and C. Marzano, *Chem. Rev.*, 2014, **114**, 815.
32 S. Tardito, O. Bussolati, F. Gaccioli, R. Gatti, S. Guizzardi, J. Uggeri, L. Marchiò, M. Lanfranchi and L. Franchi-Gazzola, *Histochem. Cell Biol.*, 2006, **126**, 473.
33 F. Dallavalle, F. Gaccioli, R. Franchi-Gazzola, M. Lanfranchi, L. Marchio, M. A. Pellinghelli and M. Tegoni, *J. Inorg. Biochem.*, 2002, **92**, 95.

34 E. W. Ainscough, A. M. Brodie, W. A. Denny, G. J. Finla, S. A. Gothe and J. D. Ranford, *J. Inorg. Biochem.*, 1999, **77**, 125.
35 Z.-C. Liu, B.-D. Wang, B. Li, Q. Wang, Z.-Y. Yang, T.-R. Li and Y. Li, *Eur. J. Med. Chem.*, 2010, **45**, 5353.
36 V. Jevtović, S. Ivković, S. Kaisarević and R. Kovačević, *Contemp. Mater.*, 2010, **I-2**, 133.
37 M. Rodic, V. Leovac, L. Jovanovic, V. Spasojevic, M. Joksovic, T. Stanojkovic, I. Matic, L. Vojinovic-Jesic and V. Markovic, *Eur. J. Med. Chem.*, 2016, **115**, 75.
38 M. Alagesan, N. S. P. Bhuvanesh and N. Dharmaraj, *Dalton Trans.*, 2013, **42**, 7210.
39 M. O. Agwara, P. T. Ndifon, N. B. Ndosiri, A. G. Paboudam, D. M. Yufanyi and A. Mohamadou, *Bull. Chem. Soc. Ethiop.*, 2010, **24**, 383.
40 J. Joseph, K. Nagashri and G. Ayisha Bibin Rani, *J. Saudi Chem. Soc.*, 2013, **17**, 285.
41 H. Liu, W. Yang, W. Zhou, Y. Xu, J. Xie and M. Li, *Inorg. Chim. Acta*, 2013, **405**, 387.
42 C.-H. Leung, S. Lin, H.-J. Zhong and D.-L. Ma, *Chem. Sci.*, 2015, **6**, 871.
43 M. R. Gill, D. Cecchin, M. G. Walker, R. S. Mulla, G. Battaglia, C. Smythe and J. A. Thomas, *Chem. Sci.*, 2013, **4**, 4512.
44 Y. Li, M. Cheng, J. Hao, C. Wang, G. Jia and C. Li, *Chem. Sci.*, 2015, **6**, 5578.
45 M. I. Sánchez, C. Penas, M. E. Vásquez and J. L. Mascareñas, *Chem. Sci.*, 2014, **5**, 1901.
46 F. E. Poynton, J. P. Hall, P. M. Keane, C. Schwarz, I. V. Sazanovich, M. Towrie, T. Gunnlaugsson, C. J. Cardin, D. J. Cardin, S. J. Quinn, C. Long and J. M. Kelly, *Chem. Sci.*, 2016, **7**, 3075.
47 L. Strekowski and B. Wilson, *Mutat. Res.*, 2007, **623**, 3.
48 K. Zhang and W. Liu, *Int. J. Electrochem. Sci.*, 2011, **6**, 1669.
49 H. Shen, X. Shao, H. Xu, J. Li and S. Pan, *Int. J. Electrochem. Sci.*, 2011, **6**, 532.
50 A. Hartwig, *Chem.-Biol. Interact.*, 2010, **184**, 269.
51 S. Kashanian, S. Askari, F. Ahmadi, K. Omidfar, S. Ghobadi and F. A. Tarighat, *DNA Cell Biol.*, 2008, **27**, 581.
52 F. Ahmadi and F. Bakhshandeh, *DNA Cell Biol.*, 2009, **28**, 527.
53 A. Mallicka, S. C. Beraa, S. Maitib and N. Chattopadhyay, *Biophys. Chem.*, 2004, **112**, 9.
54 P. B. Kandagal, S. Ashoka, J. Seetharamappa, S. Shaikh, Y. Jadegoud and O. B. Ijare, *J. Pharm. Biomed. Anal.*, 2006, **41**, 393.
55 S. F. Sun, B. Zhou, H. N. Hou, Y. Liu and G. Y. Xiang, *Int. J. Biol. Macromol.*, 2006, **39**, 197.
56 D. C. Carter and J. X. Ho, *Adv. Protein Chem.*, 1994, **45**, 153.
57 R. E. Olson and D. D. Christ, *Annu. Rep. Med. Chem.*, 1996, **31**, 327.
58 C. Bertucci and E. Domenici, *Curr. Med. Chem.*, 2002, **9**, 1463.
59 N. Janković, Z. Bugarčić and S. Marković, *J. Serb. Chem. Soc.*, 2015, **80**, 595.
60 J. Muškinja, N. Janković, Z. Ratković, G. Bogdanović and Z. Bugarčić, *Mol. Diversity*, 2016, **20**, 591–604.
61 N. Janković, J. Muškinja, Z. Ratković, Z. Bugarčić, B. Ranković, M. Kosanić and S. Stefanović, *RSC Adv.*, 2016, **6**, 39452.
62 E. López-Torres, A. R. Cowley and J. R. Dilworth, *Dalton Trans.*, 2007, 1194.
63 P. K. Larsen, *Acta. Chem., Scand. Ser. A*, 1974, **28**, 194.
64 S. X. dos Santos and É. T. G. CavalheiroII, *J. Braz. Chem. Soc.*, 2014, **25**, 1071.
65 S. Zolezzi, A. Decinti and E. Spodine, *Polyhedron*, 1999, **18**, 897.
66 B. J. Hathaway and D. E. Billing, *Coord. Chem. Rev.*, 1970, **5**, 143.
67 M. Mahajan, K. N. Saxena and C. P. Saxena, *J. Inorg. Nucl. Chem.*, 1981, **43**, 2148.
68 I. Heijenoort, *Glycobiology*, 2001, **11**, 25.
69 V. Farkaš, *Folia Microbiol.*, 2003, **48**, 469.
70 B. Pucci, M. Kasten and A. Giordano, *Neoplasia*, 2000, **2**, 291.
71 X. Huang, F. Traganos and Z. Darzynkiewicz, *Cell Cycle*, 2003, **2**, 614.
72 J. Olmsted and D. R. Kearns III, *Biochemistry*, 1977, **16**, 3647.
73 R. Lakowicz and G. Weber, *Biochemistry*, 1973, **12**, 4161.
74 W. L. Gabler, *Res. Commun. Chem. Pathol. Pharmacol.*, 1991, **72**, 39.
75 T. Topală, A. Bodoki, L. Oprean and R. Oprean, *Clujul Med.*, 2014, **87**, 215.
76 D. J. Silvaa and D. E. Kahne, *J. Am. Chem. Soc.*, 1993, **115**, 7962.
77 X. Ninga, Y. Guoa, X. Maa, R. Zhua, C. Tiana, X. Wanga, Z. Mac, Z. Zhanga and J. Liua, *Bioorg. Med. Chem. Lett.*, 2013, **23**, 3700.
78 K. A. Meadows, F. Liu, J. Sou, B. P. Hudson and D. R. McMillin, *Inorg. Chem.*, 1993, **32**, 2919.
79 J. R. Lakowicz, *Principles of Fluorescence Spectroscopy*, Kluwer Academic/Plenum, New York, 1999.
80 Agilent, *CrysAlis PRO*, Agilent Technologies, Yarnton, Oxfordshire, England, 2013.
81 G. M. Sheldrick, *Acta Crystallogr., Sect. A: Fundam. Crystallogr.*, 2008, **64**, 112.
82 M. Nardelli, *J. Appl. Crystallogr.*, 1995, **28**, 659.
83 A. L. Spek, *J. Appl. Crystallogr.*, 2003, **36**, 7.
84 C. F. Macrae, P. R. Edgington, P. McCabe, E. Pidcock, G. P. Shields, R. Taylor, M. Towler and J. van der Streek, *J. Appl. Crystallogr.*, 2006, **39**, 453.
85 NCCLS (National Committee for Clinical Laboratory Standards), *Reference Method for Broth Dilution Antifungal Susceptibility Testing of Conidium-forming Filamentous Fungi: Proposed Standard M38-P. NCCLS*, Wayne, PA, USA, 1998.
86 S. D. Sarker, L. Nahar and Y. Kumarasamy, *Methods*, 2007, **42**, 321.
87 T. Mosmann, *J. Immunol. Methods*, 1983, **65**, 55.